Avoiding Embrittlement in Heavily Stabilized β-β' Zr-Nb Alloy

PURDUE UNIVERSITY
School of Materials Engineering

Student Names: Levi Dickson, Carolina Francis, Isabella Gueth, Matthew Kaboolian
Faculty Advisors: Professor Janelle Wharry
Industrial Sponsors: Dr. Ben Eick, Mr. Brad Webb

ATI Specialty Alloys & Components is seeking to gain a greater understanding of the microstructural behavior within the Zirconium-Niobium system. As-cast and annealed microstructures at 400, 600, and 800 ℃ were quantitatively evaluated to observe recrystallization of the Zr-Nb system across multiple compositions, including 22, 59, 72, and 80 wt.% Nb. The 22 wt.% Nb grew large columnar grains with diameters greater than 0.54 mm and had slow enough cooling rates to precipitate α. Additionally, average microhardness values across the different compositions were recorded and found to be 283.6 HV and 210.7 HV for 22 wt% Nb and 72 wt% Nb, respectively.

This work is sponsored by ATI Specialty Alloys & Components, Millersburg, OR

Project Background

Goal: To expand ATI's knowledge on the control of **Zirconium-Niobium's (Zr-Nb) microstructure.** The Zr-Nb system can be thermally processed with large-scale **Vacuum Arc Remelting (VAR)** or experimental-scale **Plasma Arc Melting (PAM)**. This project attempts to answer the following questions: **can PAM be used to simulate VAR** and **how can embrittlement during forging be avoided.**

Background: The microstructure of Zr-Nb alloys have significant compositional and temperature dependences. Nb acts as a stabilizer for β-Zr grains and increases the stability of the metastable β' phase [1]. Analysis of the phase diagram shows a miscibility gap in the stable β region extending from about 22-95 wt.% Nb with maximum at peak of 71.5 wt.% Nb.

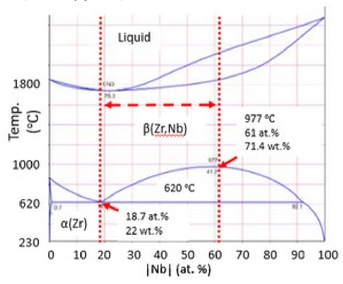

Figure 1. Annotated phase diagram of Zr-Nb binary system showing the miscibility gap and monotectoid point [2]

Challenges: Due to the **slow diffusion** there are **segregation and precipitation risks [1-3]**. The additional phases harden the alloy and when forged **lead to decreased workability and embrittlement**.

Experimental Methods

Sample & Preparation:

- *Compositions:* **22, 59, 72, 80 wt.% Nb** and **trace Hf**
- To characterize radial and vertical segregation, specimens were selectively sectioned **(see Figure 2)**
- Polished with an **attack polished at 0.5 µm colloidal silica**, etched with a **HF, HNO_3, ethanol, and 30% H_2O_2** solution

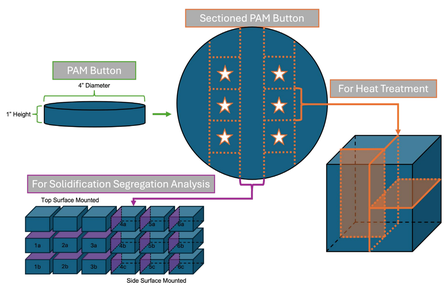

Figure 2. Diagram showing the cuts made to the buttons for each composition

Heat Treatment:
Due to **rapid and energetic oxidation of Zr** in the **presence of oxygen encapsulation** was **necessary**

1. Cubes of each composition were **encapsulated in quartz** with ½ **atm argon (see Figure 3)**
2. Samples were held at temperatures of **400, 600, and 800 °C** for **1 hour**
3. Ampules were **broken, quenched, sectioned**, and **characterized**

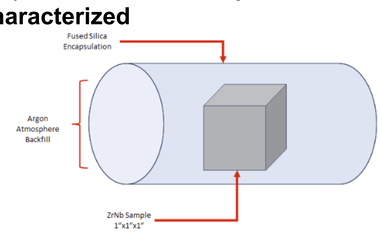

Figure 3. Diagram of encapsulated heat treatment sample

Characterization:
Optical microscopy: Canon 5D Mark III and Canon Marco Lens Ef 100mm and Olympus reflected light microscopes
SEM and EDS:

- FEI Quanta 650 for secondary and backscattered electron images.
- Phenom Pro Desktop SEM/EDS for compositional analysis

Microhardness: Vickers hardness measured for heat treated and as-cast samples using Wilson HV Tester

Figure 4. Equation for calculating the recrystallization fraction after heat treatment

$$F = 1 - \frac{(H_{measured} - H_{Rec})}{(H_{SRA} - H_{Rec})}$$

F: Recrystallization fraction
$H_{measured}$: Microhardness value of the specimen
H_{Rec}: Microhardness of the fully recrystallized sample
H_{SRA}: Microhardness of the stress-relief-annealed sample

Forging:
Cutoffs of as-cast buttons were forged through five cycles of heat to 1000 ℃, forge, reheat. Due to Zr-Nb's strength, forging experimentation was aimed at qualitative data for directing future projects.

Results & Discussion

Cutting:

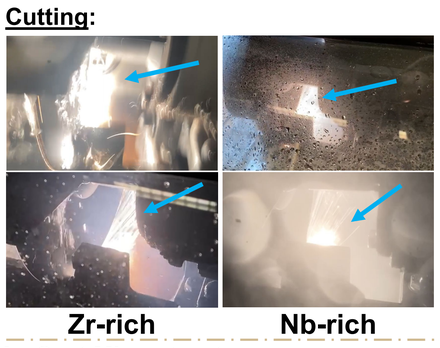

1. Significant sparking occurred while cutting with reinforced SiC
2. Color:
   1. Zr-rich → brilliant white sparks
   2. Nb-rich → muted orange-yellow sparks
3. Nb-rich's hardness, cold workability, and "gumming" led to significant wear on cutting devices

As Cast Microstructure:

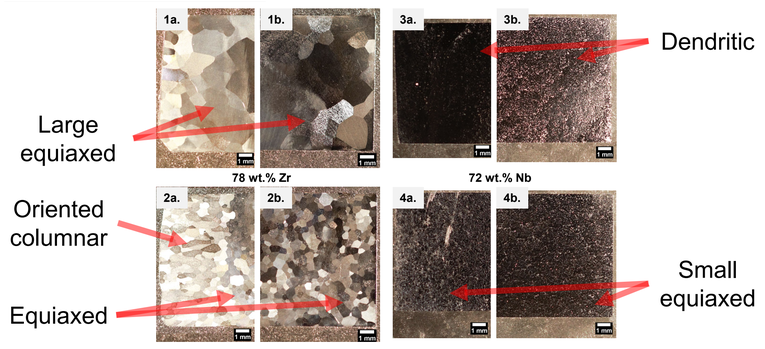

Figure 5. Optical micrographs of 78 wt.% Zr (1 & 2) and 72 wt.% Nb (3 & 4) focused on 1/3rd (bottom) and 2/3rd (top) horizontal slices. Crucible wall specimens indicated with *a* and core specimens indicated with *b*.

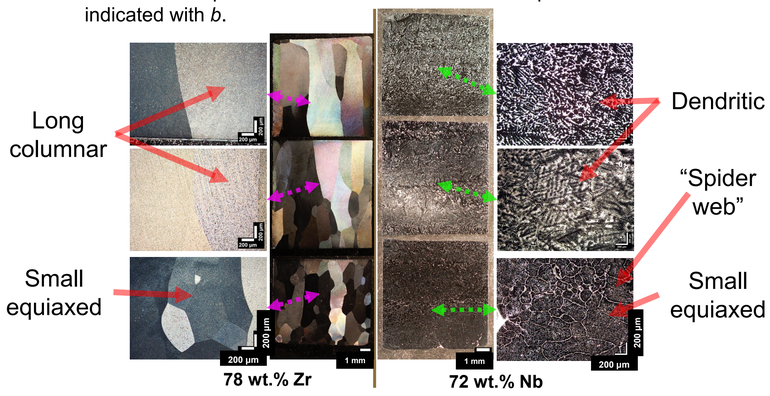

Figure 6. Vertical cross-sections between 78 wt.% Zr and 72 wt.% Nb.

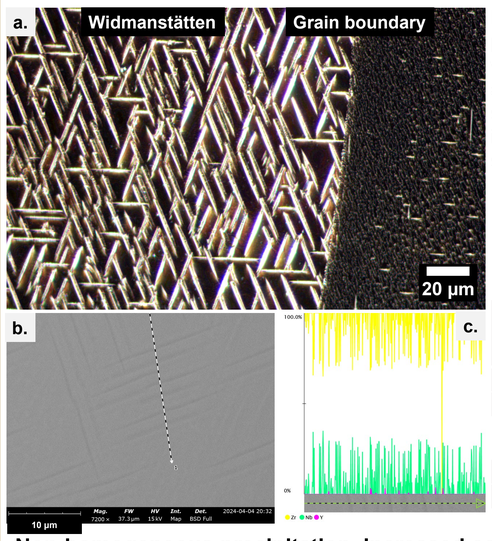

Figure 7. Widmanstätten pattern from precipitation of α within large β grains approaching of 22 wt.% Nb specimen. Optical (a), BSE image (b), line-scan EDS spectra (c).

Table 1. Average grain sizes for as-cast microstructure for 22 wt.% Nb and 72 wt.% Nb. See Figure 2. for Sample ID.

Sample ID	22 wt.% Nb Grain Size (µm)			
	1	3	4	6
a	880	916	1382	1090
b	543	360	525	658
	72 wt.% Nb Grain Size (µm)			
a	166	134	154	109
b	212	181	397	150

Non-homogeneous precipitation, increased concentration of **slowly diffusing β stabilizing elements,** and **interactions between α-platelet colonies** produce **characteristic** microstructure called **"basket weave"** structure or **Widmanstätten** structure [1].

Hardness:

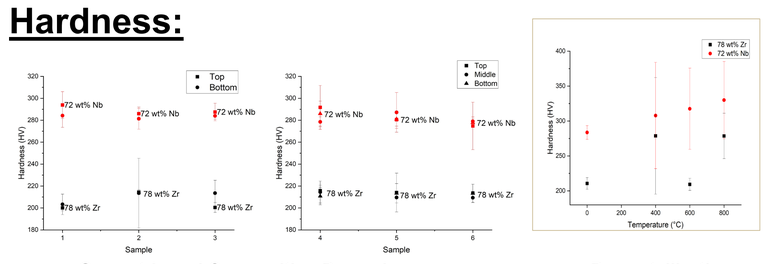

Geometric and Composition Dependence — Recrystallization

Forging:

Amount of spall increased with niobium concentration

High energy spall creates safety hazards for workers

PAM Applicability to VAR

PAM typically differ from VAR for the following reasons [4]:

1. The ATI PAM adds material as compact ingots rather than remelting overhead. Additionally, a moving plasma torch applied heat in a motion across the ingot, unlike a gaussian arc density in VAR. The plasma torch remelting can lead to a differing solidification structure, resulting in non-uniform macro segregation in the final ingot.
2. All ingots provided were in geometries that are shorter in the height:diameter ratio than typical VAR ingots, which will be most representative of the bottom, transient portion of a VAR ingot.
3. PAM ingots are prone to helium inclusions due to working with ionized gas.
4. Severe cold shuts can be seen in all samples. This can be reduced through increased heat input into the edge of the ingot, however this deviates further from simulating VAR.

Conclusions

The Zr-Nb binary exhibits significant compositional dependences of microstructure and mechanical properties:

Zr rich alloys showed:
Ease of machine

- Equiaxed chill zone in the bottom 1/3 of button volume
- Columnar grains (multi-mm in length) in remaining volume
- Slow cooling of β-grains allows precipitation of α-grains in as PAM melted buttons
- An average hardness around 210 HV, which was less than all Nb-rich compositions tested.
- Hand forging showed light spalling and sparking. Little deformation. White zirconia oxide was readily formed.

Nb rich alloys:

- Gummy and work-hardens during machining
- Equiaxed chill zone in the bottom 1/3 of button volume which switch to dendritic closer to the core and higher.
- An average hardness around 280 HV
- Heavy spalling during hand forging. Deformed more easily with better thermal recovery. Yellow niobia oxide formed following cooling.

Primarily, for the successful thermal forging of heavily stabilized Zr-Nb alloys significant post-melt reprocessing is needed.
Secondarily, due to large cooling rates, large columnar grains, and gas voids non-withdrawn PAM buttons are not completely representative of ATI's production scale VAR ingots.

Future Work

For a more completely understand and control Zr-Nb's phase behavior, the following actions should be taken:

- An **increase in compositions** would allow for a **higher resolution map** of the miscibility gap
- During heat-treatment, an expansion of **hold times and temperatures** would reveal more of the **β-β' phase interaction** as well introduction of **dynamic recrystallization to produce grain boundary α**; a phase beneficial to improve workability
- It is recommended to use **withdrawn PAM ingots in place of PAM buttons** to **simulate VAR**

Once the above is competed, determining **thermal processing parameters including compositional modelling**.

References

1. G. Lütjering and J. C. Williams, Titanium. Springer, 2010.
2. L. Pandelaers, V. Kuznetsov, and O. Zaikina, "Nb-Zr Binary Phase Diagram Evaluation,"MSI Eureka, vol. 61, 2015. doi:10.7121/msi-eureka-20.15221.1.9
3. P. E. Turchi, Thermodynamic, diffusion, and physical properties of Nb-ti-U-ZR alloys, 2018.doi:10.2172/1459146
4. In Modeling for Casting and Solidification Processing (CRC Press, 2020), pp. 627–668.

Acknowledgements

Beyond our industry sponsor and faculty advisor, the group graciously thanks the following individuals:

- **Mr. Jordan Smith** (Purdue Chemistry's Scientific Glass Blowing Lab) for his assistance in glass encapsulating samples
- **Mr. Brad Webb** (ATI) for his assistance preparing and etching samples for metallography

MSE Senior Design